

# ***Principles, Techniques, and Limitations of Near Infrared Spectroscopy***

**Marco Ferrari, Leonardo Mottola, and Valentina Quaresima**

---

## **Catalogue Data**

Ferrari, M.; Mottola, L.; and Quaresima, V. (2004). Principles, techniques, and limitations of near infrared spectroscopy. **Can. J. Appl. Physiol.** 29(4): 463-487. © 2004 Canadian Society for Exercise Physiology.

---

**Key words:** *tissue oximetry, oxidative metabolism, optical imaging, blood flow, oxygen consumption, exercise physiology*

**Mots-clés:** *oximétrie tissulaire, métabolisme oxidatif, imagerie optique, perfusion sanguine, consommation d'oxygène, physiologie de l'exercice*

## **Abstract/Résumé**

*In the last decade the study of the human brain and muscle energetics underwent a radical change, thanks to the progressive introduction of noninvasive techniques, including near-infrared (NIR) spectroscopy (NIRS). This review summarizes the most recent literature about the principles, techniques, advantages, limitations, and applications of NIRS in exercise physiology and neuroscience. The main NIRS instrumentations and measurable parameters will be reported. NIR light (700–1000 nm) penetrates superficial layers (skin, subcutaneous fat, skull, etc.) and is either absorbed by chromophores (oxy- and deoxyhemoglobin and myoglobin) or scattered within the tissue. NIRS is a noninvasive and relatively low-cost optical technique that is becoming a widely used instrument for measuring tissue O<sub>2</sub> saturation, changes in hemoglobin volume and, indirectly, brain/muscle blood flow and muscle O<sub>2</sub> consumption. Tissue O<sub>2</sub> saturation represents a dynamic balance between O<sub>2</sub> supply and O<sub>2</sub> consumption in the small vessels such as the capillary, arteriolar, and venular bed. The possibility of measuring the cortical activation in response to different stimuli, and the changes in the cortical cytochrome oxidase redox state upon O<sub>2</sub> delivery changes, will also be mentioned.*

*Dans la dernière décennie l'étude du cerveau et le muscle humain énergétique a subi un changement radical, grâce à l'introduction progressive de techniques non invasifs, y compris*

---

The authors are with the Department of Biomedical Sciences and Technologies, University of L'Aquila, 67100 L'Aquila, Italy.

*proche infrarouge (NIR) spectroscopy (NIRS). Cette revue résume la littérature la plus récente des principes, les techniques, les avantages, les limitations, et les applications de NIRS dans la physiologie d'exercice et neuroscience. Les instrumentations principales de NIRS et les paramètres mesurables seront rapportés. La lumière de NIR (700–1000 nm) pénètre des couches superficielles (la peau, subcutaneous gros, le crâne, etc.) et ou est absorbé par chromophores (oxy- et la deoxy hémoglobine et myoglobine) ou dispersé dans le tissu. NIRS est une technique non invasif et relativement bon marché optique qui devient un instrument largement utilisé pour mesurer de tissu O<sub>2</sub> saturation, les changements dans le volume d'hémoglobine et, indirectement, le flux de sang de cerveau muscle et le muscle O<sub>2</sub> consommation. Le tissu O<sub>2</sub> saturation représente un équilibre dynamique entre O<sub>2</sub> consommation de provision et O<sub>2</sub> dans les petits vaisseaux tel que le capillaire, le lit de arteriolar et venular. La possibilité pour mesurer l'activation de cortical en réponse aux stimuli différents, et les changements de l'état de redox de oxidase de cytochrome de cortical sur O<sub>2</sub> changements de livraison, seront aussi mentionnés.*

## Introduction

Starting with the pioneering work of Jobsis over 25 years ago (1977), noninvasive near-infrared (NIR) spectroscopy (NIRS) has been used first to investigate experimentally and clinically brain oxygenation, and later muscle oxidative metabolism in pathophysiology (for a review, see Boushel and Piantadosi, 2000; Boushel et al., 2001; Ferrari et al., 1997; Madsen and Secher, 1999; McCully and Hamaoka, 2000; Owen-Reece et al., 1999). In the last decade, NIRS has also been largely used to investigate the functional activation of the human cerebral cortex (for a review, see Hoshi, 2003; Obrig and Villringer, 2003). The aim of this review is to summarize the most recent literature about the principles, techniques, advantages, limitations, and applications of NIRS in exercise physiology and neuroscience.

The physical principles of NIRS have been reported previously in detail (Delpy and Cope, 1997; Rolfe, 2000; Strangman et al., 2002a). Briefly, NIR light (700–1000 nm) penetrates skin, subcutaneous fat/skull, and underlying muscle/brain, and is either absorbed or scattered within the tissue (Figure 1). The relatively high attenuation of NIR light in tissue is due to: (a) O<sub>2</sub>-dependent absorption from chromophores of variable concentration, i.e., hemoglobin (Hb), myoglobin (Mb) (in the muscle only), and cytochrome oxidase; (b) absorption from chromophores of fixed concentration (skin melanine); or (c) light scattering. Several types of NIRS equipment, based on different NIRS methods, are commercially available (Table 1). Table 2 reports the parameters measurable by NIRS. Each type of NIRS device has different characteristics, as outlined in Table 3. The choice of the NIRS device is determined by the type of information requested.

The length that light travels through the medium (optical pathlength) is longer than the distance between the source and the detector because of the scattering effects of different tissue layers. Single-distance continuous wave (CW) photometers measure only the changes in O<sub>2</sub>Hb and HHb when a constant differential pathlength factor (DPF) is included to calculate the pathlength [DPF × (source-detector separation)]. Some muscle and brain DPF values have been published (Delpy and Cope, 1997; Zhao et al., 2002). Considering that pathlength cannot change more than 10% (Ferrari et al., 1992), single-distance CW photometers mea-

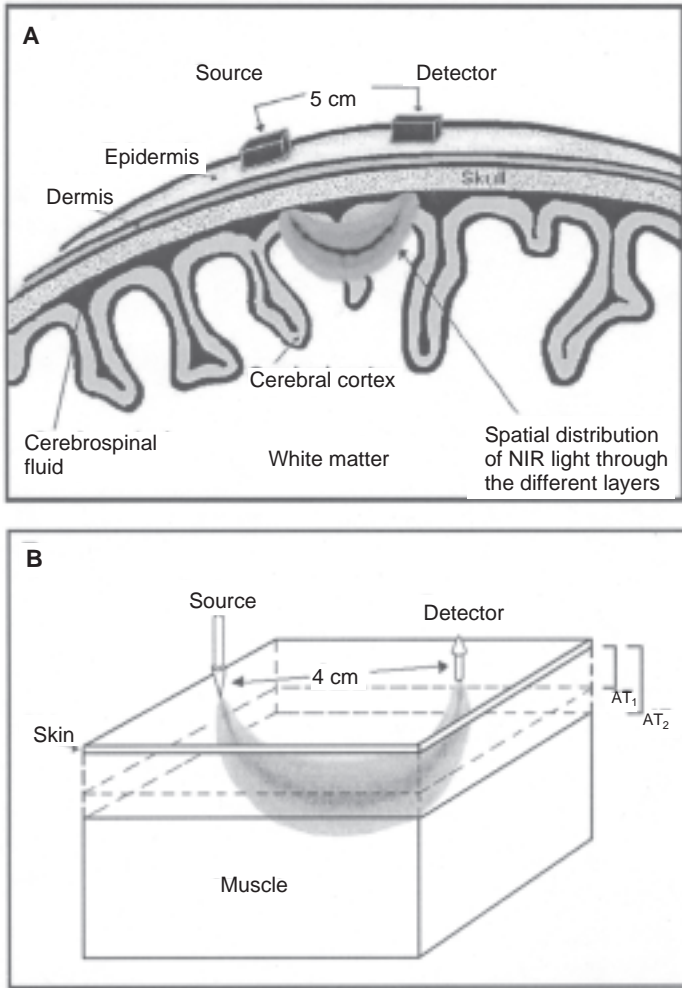


**Figure 1.** Schematic representation of NIR light traveling through (A) the head and (B) the muscle. Spatial distribution of light flux through the different tissue layers of the head or limb (due to complex light scattering) is simulated using the optical properties of skin, skull, cerebrospinal fluid (CSF), gray matter, white matter, adipose tissue, etc. The detected signal comes mainly from hemoglobin located in small vessels ( $< 1$  mm diameter) such as the capillary, arteriolar, and venular bed (or from the intracellular myoglobin in the case of the limb). Panel B indicates the penetration depth of NIR light depends on adipose tissue thickness. In particular, the light goes deeper in the muscle tissue in the case of low subcutaneous fat ( $AT_1$ ) and reaches the shallow region of the muscle tissue in the case of high subcutaneous fat ( $AT_2$ ).

**Table 1 Main NIRS Instruments**

Instrument	Technique	# of chan.	Company	Technical reference
<u>Photometers</u>				
RunMan*	Single-distance CW	1	NIM, USA	Chance et al., 1992
HEO-100*	Single-distance CW	1	OMRON, Japan	Shiga et al., 1995
NIRO-500	Single-distance CW	1	Hamamatsu, Japan	De Blasi et al., 1994
OXYMON	Single-distance CW	≥2	Artinis, Netherlands	Colier et al., 1995 van Beekvelt et al., 2002
<u>Oximeters</u>				
NIRO-300	Multi-dist. CW (SRS)	2	Hamamatsu, Japan	Suzuki et al., 1999
OM-100	Multi-dist. CW (SRS)	2	Shimadzu, Japan	Quaresima et al., 2001b
INVOS	Multi-dist. CW (SRS)	2	Somanetics, USA	Thavasoathy et al., 2002
OxiplexTS	Multi-dist. PMS	2	ISS, USA	Franceschini et al., 2002
TRS-10	TRS	1	Hamamatsu, Japan	Oda et al., 2000
<u>Imagers</u>				
ETG-100	CW	24	Hitachi, Japan	Kennan et al., 2002b
Imagent	PMS	16	ISS, USA	Wolf et al., 2002b
Monstir	TRS	32	UCL, London, UK	Hebden et al., 2002
POLIMI	TRS	8	Politecnico, Milan, Italy	Cubeddu et al., 2002
CT imager	TRS	64	Shimadzu, Japan	Hoshi et al., 2000

*Note:* CW = continuous wave; PMS = phase modulation; SRS = spatially resolved spectroscopy; \* = wearable instrument; TRS = time-resolved spectroscopy

sure quite accurately the changes in O<sub>2</sub>Hb and HHb. These instrumentations, however, cannot measure tissue O<sub>2</sub>Hb saturation. Spatially resolved spectroscopy (SRS), time-resolved spectroscopy (TRS), and phase modulation spectroscopy (PMS) can calculate tissue O<sub>2</sub>Hb saturation.

The brain/muscle volume measured by the different NIRS approaches is still controversial. However, it is generally accepted that, for a source-detector separation of 3 cm, the region of maximum brain/muscle sensitivity will be found between the source and detector fiber tip location, and roughly 1.5 cm below the surface of the skin, though a banana-shaped region of sensitivity extends both above and below this depth (Strangman et al., 2002a). Kohri et al. (2002), combining spatially- and time-resolved spectroscopy, estimated the contribution ratio of the cerebral tissue to whole optical signals at the source detector distance of 3 and 4 cm as 55 and 69%, respectively.

Different methods for NIRS signal quantification, NIRS advantages/limitations, and applications have been extensively reviewed (Boushel and Piantadosi

**Table 2 Parameters Measured Directly and Indirectly by NIRS**

Parameter	Units	Modality	MDE	Reference
$\Delta$ O <sub>2</sub> Hb	A.U., $\mu\text{M}\times\text{cm}$ ,	D	yes	Delpy and Cope, 1997
$\Delta$ HHb	$\mu\text{M}$		yes	Delpy and Cope, 1997
$\Delta$ tHb			yes	Delpy and Cope, 1997
OI			yes	Grassi et al., 1999
Tissue O <sub>2</sub> saturation	%	D (by SRS) D (by PMS) D (by TRS)	yes yes yes	Quaresima et al., 2002b Franceschini et al., 2002 Oda et al., 2000
sVO <sub>2</sub>	%	I (by VOM) D	no no	Yoxall et al., 1997 Franceschini et al., 2002
Muscle BF	$\text{ml}\cdot 100\text{ml}^{-1}\cdot\text{min}^{-1}$	I (by VOM) I (by ICG)	no yes	De Blasi et al., 1994 Boushel et al., 2000b
Muscle VO <sub>2</sub>	$\text{ml}\cdot 100\text{g}^{-1}\cdot\text{min}^{-1}$	I (by VOM) I (by AOM)	no no	De Blasi et al., 1994 De Blasi et al., 1993
Recovery time Muscle	seconds	D	no	Chance et al., 1992
compliance	$\text{ml}\cdot\text{L}^{-1}\cdot\text{mmHg}^{-1}$	I	no	Binzoni et al., 2000
Cerebral BV	$\text{ml}\cdot 100\text{ml}^{-1}$	I (by O <sub>2</sub> swing)		Owen-Reece et al., 1999
Cerebral BF	$\text{ml}\cdot 100\text{ml}^{-1}\cdot\text{min}^{-1}$	I (by O <sub>2</sub> swing) I (by ICG)		Owen-Reece et al., 1999 Owen-Reece et al., 1999

*Note:*  $\Delta$  = relative changes from zero; tHb =  $\Delta$  O<sub>2</sub>Hb +  $\Delta$  HHb; OI = oxygenation index ( $\Delta$  O<sub>2</sub>Hb -  $\Delta$  HHb); MDE = measurable during exercise; sVO<sub>2</sub> = venous O<sub>2</sub> saturation; BF = blood flow; BV = blood volume; VO<sub>2</sub> = oxygen consumption; A.U. = arbitrary units; D = directly; I = indirectly; SRS = spatially resolved spectroscopy; PMS = phase modulation spectroscopy; TRS = time resolved spectroscopy; VOM = venous occlusion method; AOM = arterial occlusion method; ICG = indocyanine green.

2000; Boushel et al., 2001; Ferrari et al., 1997; McCully and Hamaoka, 2000; Strangman et al., 2002a). Briefly, the main limitations of NIRS measurements are due to: (a) the interference of skull thickness or adipose tissue thickness (ATT) on brain or muscle measurements, respectively; (b) the controversial unknown contribution of myoglobin to the muscle NIRS signal; (c) the effect of blood volume changes on the tissue pathlength, and then on the observed sample volume; (d) the difficulty of predicting how much of an observed NIRS signal change is due to brain vs. scalp blood flow, or (e) simultaneous changes in flow and volume.

In a recent theoretical study of light propagation in adult head models by using a Monte Carlo simulation, Okada and Delpy (2003) studied the effect of the superficial tissue thickness on the partial optical pathlength in the brain and on the

**Table 3 Characteristics of NIRS Devices**

	Single-distance CW Photometers		1–2 Channel Oximeters			Imagers		
	changes #	changes #	SRSCW	PMS	TRS	CW	PMS	TRS
[O <sub>2</sub> Hb], [HHb], [tHb] (μM)				absolute value	absolute value	changes #	absolute value	absolute value
Scattering & absorption coefficient and pathlength measurement	no	no	yes	yes	yes	no	yes	yes
Tissue O <sub>2</sub> Hb saturation (SO <sub>2</sub> , %)	no	yes	yes	yes	yes	no	yes	yes
Penetration depth with a 4-cm source-detector separation	low	low, deeper for SO <sub>2</sub>	deep	deep	deep	low	deep	deep
Sampling rate (Hz)	≤100 Hz	≤6 Hz	≤100 Hz	≤6 Hz	≤6 Hz	≤100 Hz	≤50 Hz	1 Hz
Spatial resolution (cm)	n.a.	n.a.	n.a.	n.a.	n.a.	≤0.5 cm	≤0.5 cm	≤0.5 cm
Instrument size	very small	small	small	medium	medium	bulky	bulky	bulky
Instrument stabilization	no	no	no	required	required	no	no	required
Transportability	easy	easy	easy	easy	easy	feasible	feasible	feasible
Instrument cost	low	moderate	moderate	moderate	high	very high	very high	very high
Caution for eye exposure to coherent sources	no	no	no	no	yes	yes	yes	yes
Stable optical contact	critical	good	good	good	good	critical	good	good
Precise anatomical localization	no	no	no	no	no	scarce	scarce	scarce
Telemetry	feasible	feasible	feasible	not easy	not easy	not easy	not easy	not easy
Discrimination between cerebral and extracerebral tissue (scalp, skull, CSF)	n.a.	n.a.	feasible	feasible	feasible	n.a.	feasible	feasible
Possibility to measure deep brain structures on newborns	feasible	feasible	feasible	feasible	feasible	feasible	feasible	feasible

*Note:* CSF = cerebrospinal fluid; CW = continuous wave; n.a.= not available; PMS = phase modulation spectroscopy; SRS = spatially resolved spectroscopy; tHb = O<sub>2</sub>Hb+HHb; TRS = time resolved spectroscopy; # = when differential pathlength factor (DPF) is included to calculate the tissue pathlength [= DPF × (source-detector separation)].

spatial sensitivity profile. The mean optical pathlength (measurable by time-resolved spectroscopy and phase modulation spectroscopy) increases when the skull thickness increases, whereas the partial mean optical pathlength in the brain decreases when the skull thickness increases. The partial optical pathlength (at a source-detector distance of 3 cm) depends mainly on the depth of the inner skull surface whereas the spatial sensitivity profile is significantly affected by the thickness of the cerebrospinal fluid layer. Moreover, an analysis was developed by another group for changes in mean time of flight (instead of changes in attenuation) to reduce the cross talk for the layers of cortical activation (Uludag et al., 2002).

The influence of ATT on light propagation in leg muscles has been examined by a diverse number of researchers. More recently, Matsushita et al. (1998) concluded that NIR light penetrates shallow regions of muscle under the skin and subcutaneous fat even when the ATT is 1.5 cm.

The NIRS technique is unable to differentiate between the signal attenuation due to Hb and Mb because the absorbency signals of these two chromophores overlap in the NIR range. Within a given volume of muscle there are differences in concentration of both Hb and Mb and in their binding capacities (i.e., Hb has four times more oxygen binding sites than Mb). Little data is available on the Hb/Mb ratio in the human muscles. On the basis of these studies, Mb is on average 4 mg/g wet tissue in human gastrocnemius (Mancini et al., 1994) and 4.5 mg/g in vastus lateralis (Masuda et al., 1999). Although the NIRS sample volume is unknown, considering a muscle blood volume of about 10% one can estimate its weight as a confounding factor at 10% of the whole Hb signal, an amount that may be considered negligible.

Tran et al. (1999) first demonstrated by  $^1\text{H}$ -magnetic resonance spectroscopy (MRS) that oxy-Mb desaturation kinetics matches the NIRS signal. Richardson et al. (2002) found that at rest the intramuscular  $\text{O}_2$  stores (measured by the appearance of  $^1\text{H}$ -MRS -deoxy-Mb signal during suprasystolic cuff occlusion) begin to decrease after 4 min, and that maximal Mb desaturation is achieved after 8 min. Conversely, at rest the intramuscular  $\text{O}_2$  stores, as measured by NIRS during suprasystolic cuff occlusion, begin to decrease immediately after the beginning of the occlusion and the maximal desaturation is achieved after 5–6 min (Komiya et al., 2001). During high intensity exercise, Mb typically desaturates to only 50% of the level attained during cuff occlusion (Wittenberg & Wittenberg, 2003), and muscle oxygenation, as measured by CW NIRS, typically desaturates to about 90% of the level attained during the cuff occlusion (Grassi et al., 2003).

Overall these data would suggest that, in the case of a short quadriceps maximal voluntary contraction, the measured value of the vastus lateralis  $\text{O}_2$  saturation reflects predominantly (at least 80%) the weighted mean of arteriolar, capillary, and venular  $\text{O}_2\text{Hb}$  saturation. The remainder can be attributed to the contribution of Mb oxygen saturation. Nevertheless, more combined  $^1\text{H}$ -MRS and NIRS studies are needed to clarify not only the issue of the contribution of Mb to the NIRS signal, but also the kinetics and the amount of Mb desaturation during exercises with different workloads (Conley et al., 2000).

As discussed by McCully and Hamaoka (2000), not all published studies found a good correlation between muscle oxygenation by NIRS and venous blood  $\text{O}_2$  saturation (Costes et al., 1996; Hicks et al., 1999; MacDonald et al., 1999).



During a prolonged exercise, venous blood O<sub>2</sub> saturation initially decreased but did not increase as muscle oxygenation did. McCully and Hamaoka proposed several possible explanations, i.e., change in the calibration curve due to blood volume changes, and a shift of the weighted average of the NIRS signal toward capillaries. In support of the effect of apparent sample volume during prolonged exercise, some studies have shown that the magnitude of the partial recovery in muscle oxygenation during exercise was reduced during hypoxia (Costes et al., 1996; MacDonald et al., 1999). This is because during hypoxia the overall O<sub>2</sub> saturation and the gradients along the vascular trees are reduced, and thus the shifts in blood volume between compartments will affect fewer NIRS measurements (McCully and Hamaoka, 2000).

### **NIRS Instrumentation and Measurable Parameters**

Several types of NIRS equipment, based on different NIRS methods, are commercially available (Table 1). The advantages and disadvantages of the different NIRS approaches have been reviewed (Delpy and Cope, 1997; Hoshi, 2003; Rolfe, 2000; Strangman et al., 2002a). Most of the commercial instruments utilize CW light in combination with a modified Lambert-Beer law (Delpy and Cope, 1997) to measure changes in O<sub>2</sub>Hb and HHb (Figure 2). In a scattering medium such as biological tissue, quantification of the NIRS signal is difficult and different methods have been proposed; one of the most reliable is the spatially resolved spectroscopy (SRS). SRS and time/phase-resolved instruments are the only ones to provide the measurement of average tissue O<sub>2</sub> saturation.

In SRS, which uses CW light and a multidistance approach, the slope of NIR light attenuation vs. distance is measured at a distant point from the light input, from which the absolute ratio of O<sub>2</sub>Hb to the total Hb content (tHb), and hence average tissue O<sub>2</sub> saturation (SRS-O<sub>2</sub>), can be calculated using the photon diffusion theory (Suzuki et al., 1999). SRS-O<sub>2</sub> represents a dynamic balance between O<sub>2</sub> supply and O<sub>2</sub> consumption in tissue capillaries, arterioles, and venules, because in larger blood vessels NIR light is fully absorbed by the high hemoglobin concentration. From anatomical studies of the brain, the ratio of venule to total vessel volume ranges from 2/3 to 4/5 (van Lieshout et al., 2003). Because about 5% of the blood is in the capillaries and about 20% in the arterioles, NIRS measures mainly the local venous O<sub>2</sub>Hb saturation.

NIRS instruments have been validated *in vivo* by several researchers using different experimental modalities. Boushel et al. (2001) found that SRS-O<sub>2</sub> of the vastus lateralis was inversely related with the femoral arterio-venous O<sub>2</sub> (a-vO<sub>2</sub>) difference during dynamic knee extension exercise in normoxia, hypoxia, and hyperoxia.

Recently several groups have begun to use multichannel CW imaging systems that allow the generation of images of a larger area of the subject's head and muscle with high temporal resolution (up to 10 Hz), and thereby the production of maps of cortical and muscle oxygenation changes (Miura et al., 2001; Obrig and Villringer, 2003; Quaresima et al., 2001a, 2002a). The noninvasive cortical NIR images can be obtained in straightforward setups that can be easily combined with other functional methods, in particular EEG. Multichannel brain NIR imaging has



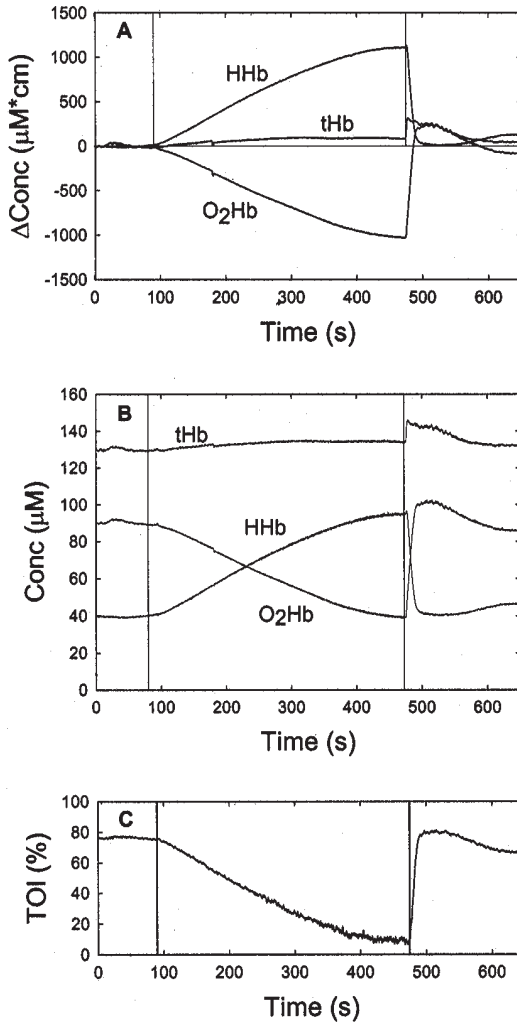


**Figure 2.** Typical time course of brachioradialis muscle oxygenation measured during arterial occlusion by different NIRS technologies: (A) single-distance continuous wave spectroscopy; (B) phase modulation spectroscopy and/or time resolved spectroscopy; and (C) spatially resolved spectroscopy. Vertical lines indicate the duration of arterial occlusion provoked inflating (250 mmHg) the cuff positioned around the arm. Time course of concentration changes (expressed in  $\mu\text{M}\cdot\text{cm}$ , when DPF is not included) in O<sub>2</sub>Hb, HHb, and tHb measured by single-distance continuous wave photometers (Panel A). Time course of tissue O<sub>2</sub> saturation (TOI, %) measured by continuous-wave spatially resolved spectroscopy, phase-modulation spectroscopy, and time-resolved spectroscopy (Panel C). Time course of absolute concentration (expressed in  $\mu\text{M}$ ) of O<sub>2</sub>Hb, HHb, and tHb measured only by phase modulation spectroscopy and time resolved spectroscopy (Panel B).

two major advantages: it can address issues concerning neurovascular coupling in the human adult, and can extend functional imaging approaches to the examination of the diseased brain. Unfortunately, there are few commercially available imagers, they are quite expensive, and most of them lack U.S. Food and Drug Administration approval.

Although many interesting studies have been performed with multichannel CW systems, the lack of pathlength determination limits the accuracy of the results (Ferrari et al., 1992). Imagent (ISS Inc., Urbana, IL) is a new device that allows the measurement of O<sub>2</sub>Hb and HHb concentration maps in tissue via phase modulation. The device works by emitting NIR light into tissue at known distances from a detector. Light of two different wavelengths is used and the light is modulated at a radio frequency of 110 MHz. The collected light is measured and processed and the absorption and scattering coefficients of the medium are determined. Once the absorption and scattering are determined, the assumption that Hb is the only significant absorber is applied and the O<sub>2</sub>Hb and HHb concentrations are calculated.

Absolute concentrations of O<sub>2</sub>Hb and HHb also can be measured by TRS. For this purpose, a number of companies and academic institutions have been developing multichannel TRS systems (Cubeddu et al., 2002; Hillman et al., 2001; Hoshi et al., 2000). Recently, an 8-channel portable instrument based on TRS has been developed and tested for monitoring spatial changes in calf O<sub>2</sub>Hb saturation during dynamic plantar flexion exercise with a sampling time of 200 ms (Cubeddu et al., 2002). A 32-channel TRS optical imaging instrument has been developed by the University College of London principally to study functional parameters of the brain of a newborn (Hillman et al., 2001). Images representing the internal scattering and absorbing properties of the arm, as well as images revealing physiological changes during a simple finger flexion exercise, were presented (Hillman et al., 2001). 3-D images of the newborn infant brain with a cerebral haemorrhage predominantly located within the left ventricle have recently been generated (Hebden et al., 2002).

However, there is a number of tradeoffs when using these multichannel systems, including poor spatial resolution (about 5 mm), difficulty with precise anatomical localization, and relatively poor penetration and localization depth. All the parameters measurable directly and indirectly by the NIRS devices, based on different approaches, are reported in Table 2.

#### MUSCLE O<sub>2</sub> CONSUMPTION (VO<sub>2</sub>) AND BLOOD FLOW (BF)

The utility to measure VO<sub>2</sub> has also been demonstrated. For example, VO<sub>2</sub> can be measured in the arm or in the leg by calculating the rate of conversion of O<sub>2</sub>Hb to HHb during a period of tourniquet-induced ischemia (De Blasi et al., 1993). VO<sub>2</sub> can be measured at rest and during forearm maximal voluntary contraction (MVC) achieved with and without vascular occlusion. The MVC, performed during vascular occlusion, caused a complete desaturation in 10–15 sec, which was not followed by any further desaturation when the second contraction was performed. No difference was found in VO<sub>2</sub> measured during MVC with and without vascular occlusion. The relationship between VO<sub>2</sub> in the soleus muscle and the level of isometric exercise expressed as % of MVC was investigated by Colier et al. (1995).

A linear relationship was found between the  $\text{VO}_2$  and the level of exercise. More recently, Sako (2001) examined the validity of the  $\text{VO}_2$  method. Subjects performed two bouts of dynamic handgrip exercise, once for the NIRS measurement and once for the  $^{31}\text{P}$ -MRS measurement as a standard. There was a physiologically significant correlation ( $r = 0.965$ ) between the  $\text{VO}_2$  values measured by the two methods.

Several recent studies have suggested that the NIRS  $\text{VO}_2$  method could be useful not only for examining regional differences, but also changes over time between muscle groups as a function of training. NIRS in combination with  $^{31}\text{P}$ -MRS was used to assess muscle bioenergetics (Binzoni et al., 1998; Boushel et al., 1998). Energy metabolism and interstitial fluid displacement were studied in the human gastrocnemius during three subsequent 5-min ischaemia-reperfusion periods (Binzoni et al., 1998).  $\text{VO}_2$  in the muscle region of interest, as estimated by NIRS, was approximately  $8 \mu\text{mol}/100\text{g}/\text{min}$ . Phosphocreatine (PCr) and ATP concentrations did not change over the whole experimental period. Forearm flexor muscle  $\text{VO}_2$  was measured during ischemia at rest and rhythmic handgrip at 15% and 30% of MVC, postexercise muscle ischaemia, and recovery (Boushel et al., 1998). The oxygenation of the forearm flexor muscles closely reflected the exercise intensity and metabolic rate determined by  $^{31}\text{P}$ -MRS, but not the rate derived from flow and the  $a\text{-vO}_2$  difference.

As suggested by Boushel et al. (1998), this discrepancy is due to the limitations in sampling venous blood representative of the flexor muscle capillaries. Using  $^{31}\text{P}$ -MRS and NIRS simultaneously, it was found that the initial rate of finger flexor deoxygenation during immediate postexercise ischemia (exercise: 5-min submaximal isotonic grip exercise at 10–40% of MVC) was a reflection of muscle  $\text{VO}_2$  (Hamaoka et al., 1996).

NIRS has also been successfully applied for the simultaneous measurement of forearm BF (FBF) and  $\text{VO}_2$  ( $\text{FVO}_2$ ) by inducing a 50-mmHg venous occlusion (De Blasi et al., 1994). FBF data were validated by strain-gauge plethysmography (De Blasi et al, 1994; Homma et al., 1996). Therefore, NIRS provides the particular advantage of obtaining the concomitant evaluation of FBF and  $\text{FVO}_2$ , allowing a correlation between these two variables by a single maneuver without discomfort for the subject. The  $\text{FVO}_2$  values obtained by using the venous occlusion method correlated with the  $\text{FVO}_2$  values obtained by using the arterial occlusion method ( $r^2 = 0.66$ ,  $p < 0.01$ ) (De Blasi et al., 1997).  $\text{VO}_2$  and BF in resting and exercising forearm (sustained isometric handgrip exercise) were examined via NIRS and the results were compared with those via the global muscle  $\text{VO}_2$  data and FBF derived from the Fick method and plethysmography (van Beekvelt et al., 2001b). This study concluded that NIRS is an appropriate tool for providing information about local  $\text{VO}_2$  and local FBF because both place and depth of the NIRS measurements reveal local differences that are not detectable by the more established, but also more global, Fick method.

These methods were also successfully used to estimate FBF and  $\text{FVO}_2$  during venous occlusion imposed at rest and immediately after handgrip exercise with incremental loads (5–30% of MVC) (Homma et al., 1996). Quantitative measurements of regional muscle BF at rest and during exercise were also possible using NIRS and a light-absorbing tracer, indocyanine green (ICG). This invasive method

has been applied to evaluate the circulatory responses to exercise along with the assessment of SRS-O<sub>2</sub> (Bangsbo et al., 2000; Boushel et al., 2000a, 2000b).

#### OTHER PARAMETERS MEASURABLE ON MUSCLES

Muscle venous saturation (SvO<sub>2</sub>) can be estimated with NIRS by applying a venous occlusion and measuring changes in O<sub>2</sub>Hb vs. tHb (Yoxall et al., 1997). More recently, another method for the measurement of SvO<sub>2</sub>, based on the respiration-induced oscillations of the NIR absorption in tissues, has been reported (Franceschini et al., 2002). In the vastus medialis and vastus lateralis muscles, a good agreement was found between SvO<sub>2</sub> measured with the new method and SvO<sub>2</sub> measured with the venous occlusion method (average deviation of 0.8%).

The recovery time reflects the balance of O<sub>2</sub> delivery and O<sub>2</sub> demand in the localized muscles following muscle work, and it can be interpreted as a measure of the time for repayment of O<sub>2</sub> and energy deficits accumulated during intense exercise by tissue respiration under ADP control (Chance et al., 1992). Recovery time can be measured also after tourniquet-induced ischemia (McCully et al., 1994; Sahlin, 1992). McCully et al. (1994) investigated simultaneously PCr and muscle oxygenation during the recovery phase from isokinetic plantar flexion. Muscle reoxygenation approximated submaximal PCr recovery and was not different between maximal and submaximal exercise, demonstrating that <sup>31</sup>P-MRS measurements of PCr recovery and NIRS measurements of recovery of muscle oxygenation provide similar information.

A method has been developed to measure the compliance of the microvascular superficial venous system of the lower limb by NIRS (Binzoni et al., 2000). This method is complementary to strain-gauge plethysmography, which does not allow compliance to be distinguished between deep and superficial venous or between venous and arterial compartments. Hydrostatic pressure (P) changes were induced in a calf region of interest by head-up tilt of the subject from alpha = -10 to 75 deg. For P ≤ 24 mmHg, the measured compliance, based on NIRS data of tHb, HHb, and O<sub>2</sub>Hb, reflects essentially that of the superficial venous system. For P ≥ 24 mmHg, no distinction can be made between arterial and venous volume changes. However, by following the changes in O<sub>2</sub>Hb and HHb in the P range from -16 to 100 mmHg, it seems possible to assess the characteristics of the vasomotor response of the arteriolar system. These results were later explained by Binzoni et al. (2003) in a study in which it was demonstrated (via a NIRS dye dilution technique) that a reduction in blood flow is responsible for the limited O<sub>2</sub>Hb concentration increase during the tilting maneuver from 0 to 60 deg.

Since adipose tissue interacts with the NIR light, the monitored muscle oxygenation changes are underestimated if adipose tissue thickness is not taken into consideration. There are reports demonstrating that adipose tissue affects *in vivo* quantitative NIRS, especially BF and VO<sub>2</sub> in skeletal muscle (van Beekvelt et al., 2001a). A negative correlation was found between VO<sub>2</sub> and adipose tissue thickness (also Binzoni et al., 1998). No correlation was found between MVC and VO<sub>2</sub>, nor between MVC and adipose tissue thickness, indicating that the contraction force did not confound the results. The main conclusion of these studies was that adipose tissue thickness has a substantial confounding influence on *in vivo* NIRS measurements, and that it is essential to incorporate this factor into NIRS muscle

studies in order to justify comparisons between different muscle groups. Recently an algorithm capable of correcting for the influence of the subcutaneous fat layer has been proposed (Niwayama et al., 2000); however, it is not included in the commercial units.

#### TISSUE OXIMETRY

Madsen and Secher (1999) reviewed brain oximetry studies based on NIRS. Caveats of cerebral oximetry include insufficient light shielding, optode displacement, and a sample volume including muscle or the frontal sinus mucous membrane. The relative influence from the extracranial tissue is minimized by optode separation and correction for an extracranial sample volume, or both. The natural pigment melatonin and also water are of little influence to spectroscopic analysis of cerebral oxygenation, whereas bilirubin systematically lowers brain oxygenation and attenuates the detection of changes in cerebral oxygenation. The application of intracranial NIRS in adults has been hampered by concerns over contamination from extracranial tissues.

A typical SRS system like the NIRO-300 (Hamamatsu Photonics, Hamamatsu City, Japan) provides continuous online measurements of  $O_2Hb$  and  $HHb$  concentration changes and a calculated tissue  $O_2$  saturation named TOI. Al-Rawi et al. (2001) confirmed the anatomic source of TOI in the adult cranium on patients undergoing carotid endarterectomy. A change in TOI was predominantly associated with internal carotid artery clamping. When TOI changed during external carotid artery clamping, there were significant changes in blood pressure, or extracranial-to-intracranial anastomosis was evident. In the absence of such variables, the sensitivity of TOI to intracranial and extracranial changes was 87.5% and 0%, respectively, and specificity was 100% and 0%, respectively.

Two SRS oximeters, NIRO-300 and OM-200 (Shimadzu, Tokyo, Japan), were compared with regard to the measurement of  $O_2$  saturation values in two forearm muscle groups at rest and during arterial occlusion. There was a significant correlation between the muscle  $O_2$  saturation values obtained at rest using the two oximeters, whereas these values were significantly different during arterial occlusion (Komiyama et al., 2001). Thus, although there was good agreement between muscle  $O_2$  saturation values measured using the two oximeters, the operating range (i.e., the interval within which the instrument works reliably) of the tissue oximeters should be recognized and indicated. Thavasoathy et al. (2002) compared the cerebral cortex oxygenation as measured by the NIRO-300 and the INVOS 5100 (Somanetics, Troy, MI). Both monitors demonstrated similar changes in response to hyperoxia and hypocapnia (coefficient of variance for  $FiO_2$  0.45 = 10.0%,  $FiO_2$  1.0 = 10.1%, hypocapnia = 14.5%).

Cerebral oximetry found several interesting clinical and physiological applications (for a review, see Madsen and Secher, 1999). For example, van Lieshout et al. (2003) investigated cerebral oxygenation during syncope, and Imray et al. (1998) studied cerebral regional  $O_2$  saturation in subjects ascending rapidly to 4,680 m. Also muscle oximetry found several interesting applications. For example, Boushel et al. (2000a) investigated calf and peritendinous oxygenation during dynamic exercise, and Quaresima et al. (2002b) studied oxygen resaturation of thigh and calf muscles after two treadmill stress tests.

## CORTICAL CYTOCHROME OXIDASE REDOX STATE

NIRS assessment of the redox state of mitochondrial cytochrome oxidase  $\text{Cu}_A$  could be a valuable technique for monitoring intracellular  $\text{O}_2$  delivery. Although the NIRS hardware has been refined and the algorithms (used to deconvolute the light absorption signal) have been improved, recent years have seen lively discussion in the literature on the possibility of measuring cortical cytochrome oxidase by NIRS. Conversely, this measurement cannot be done on muscle tissue because of the Mb interference. Hoshi (1997) found in rats that  $\text{O}_2$ -dependent redox changes in cytochrome oxidase occur only when  $\text{O}_2$  delivery is extremely impaired.

To improve the accuracy of this measurement, most of the recent studies employed a multiwavelength detector. Quaresima et al. (1998) determined the relationship between the redox state of mitochondrial cytochrome oxidase  $\text{Cu}_A$  and Hb oxygenation on newborn piglet brain. The large reductions in the  $\text{Cu}_A$  redox state during anoxia ( $1.8 \mu\text{M}$ ) were caused by a decrease in the rate of  $\text{O}_2$  delivery to the cytochrome oxidase  $\text{O}_2$  binding site; the small oxidations ( $0.2 \mu\text{M}$ ) during hypercapnia were likely due to the effects of metabolic changes on the redox state of  $\text{Cu}_A$  rather than to increases in the rate of  $\text{O}_2$  delivery. In the same experimental animal model, Cooper et al. (1999) used mitochondrial inhibitors (cyanide) to demonstrate that cytochrome oxidase NIRS can measure mitochondrial dysfunction. The  $\text{O}_2$  dependency and precision of cytochrome oxidase signal from full spectral NIRS of the piglet brain was measured during brief anoxic swings at both normocapnia and hypercapnia (Springett et al., 2000a). A minimal interference between the Hb and  $\text{Cu}_A$  signals was found in this model, the  $\text{Cu}_A$  oxidation state was independent of cerebral oxygenation at normoxia, and the oxidation after hypercapnia was not the result of increased cerebral oxygenation.

Changes in Hb oxygenation and oxidation state of cytochrome oxidase were measured simultaneously with phosphorus metabolites using  $^{31}\text{P}$ -MRS by applying a transient anoxia (Springett et al., 2000b). During the onset of anoxia, there was no change in either PCr concentration or the oxidation state of the  $\text{Cu}_A$  centre of cytochrome oxidase until a substantial fall in cerebral Hb oxygenation occurred, at which point the  $\text{Cu}_A$  centre reduced simultaneously with the decline in PCr. The concomitant reduction of  $\text{Cu}_A$  and decline in PCr can be explained in terms of the effects of the falling mitochondrial electrochemical potential. From these observations it was concluded that, at normoxia, oxidative phosphorylation and the oxidation state of the components of the electron transport chain are independent of cerebral oxygenation, and that the reduction in the  $\text{Cu}_A$  signal occurs when  $\text{O}_2$  tension limits the capacity of oxidative phosphorylation to maintain the phosphorylation potential.

De Visscher et al. (2002) demonstrated that nitric oxide does not inhibit cerebral cytochrome oxidase after brief anoxia or during reoxygenation after a brief anoxic period. Although these are very interesting results, the validity of the cytochrome signal has been questioned as it could easily be overwhelmed by the Hb signal. Using a piglet model, Sakamoto et al. (2001) found that the cytochrome signal as presently measured by scanning NIRS is highly dependent on hema-tocrit.

Several human visual cortex cytochrome oxidase studies have been performed by the Villringer's group. For example, Wobst et al. (2001) investigated the vascu-



lar and metabolic response to brain activation in human primary and adjacent secondary visual cortex. Using NIRS they were able to measure concentration changes in the redox status of the cytochrome-c oxidase. Predictions of cellular and vascular oxygenation responses to visual stimulation were good for 6- to 24-s stimuli duration under the assumption of a linear transfer characteristic.

#### CEREBRAL BLOOD FLOW AND CEREBRAL BLOOD VOLUME

Methods of using NIRS to achieve absolute quantification of cerebral blood flow (CBF) and cerebral blood volume (CBV) by a transient hypoxia have been developed in neonatal intensive care and have also been applied in adults (see Owen-Reece et al., 1999, for a review). However, these methods were questioned because, for example, they give systematically different CBV readings and large intersubject variability (see Newton et al., 1997; van de Ven et al., 2001; Wolf et al., 2002a). Therefore, these methods have found a scarce application in clinics. Roberts (1998) described a novel noninvasive method for repeatedly measuring CBF during cardiopulmonary bypass on children with NIRS using ICG, injected into the bypass circuit, as an intravascular tracer. The method was compared with microsphere injection in piglets undergoing cardiopulmonary bypass.

More recently, CBF was estimated using NIRS and pulse dye-densitometry after intravenous ICG injection (Gora et al., 2002). Arterial and cerebral changes in ICG concentration were measured using pulse dye-densitometry and NIRS, respectively. The precision was improved using a deconvolution algorithm (coefficient of variation of 10.1%). The precision of this method has been improved by applying the Fick principle in both integral and differential forms using a linear regression technique to improve the precision of calculated values of CBF (Springett et al., 2001). In addition, the differential method allowed the venous outflow to be calculated, giving further information on the state of the capillary bed.

The same group (Brown et al., 2002) more recently has developed a method that allows, after ICG injection, quantitative measurement of CBF, CBV, and mean transit time (MTT). Measurements of CBF, CBV, and MTT were made on piglets in normocapnia, hypocapnia, and hypercapnia to test the technique over a range of hemodynamic conditions. The accuracy of the new approach has been determined by direct comparison with measurements made using a computed tomography technique. No significant difference was found between computed tomography and NIRS measurements of CBF, CBV, and MTT (Brown et al., 2002).

Hopton et al. (1999) developed an integration method to measure CBV in adults by using ICG. After bolus injection, concentration-time integrals of cerebral tissue ICG concentration measured by NIRS were compared with corresponding integrals of the cerebral blood ICG concentrations estimated by high-performance liquid chromatography of peripheral blood samples. Multichannel NIRS with ICG was preliminarily used to measure regional CBF in the temporal lobes of infants (Kusaka et al., 2001). Since the application of ICG in the adult human critically depends on differentiation between extra- and intracerebral vascular compartments, Kohl-Bareis et al. (2002) investigated the latency and shape of the change in absorption of a bolus of ICG traveling through the cerebral vasculature using frequency-domain and multidistance measurements. Based on measurements of both



the photon's mean time of flight (phase) and the intensity, the results revealed the differentiation between an upper layer (skin and skull) and a lower layer (brain). The bolus in the deeper tissue layers had a peak of about a 10-s width, while the change in absorption in the upper layers shows a much longer recovery time. This was in qualitative agreement with magnetic resonance imaging results using a gadolinium bolus (Kohl-Bareis et al., 2002).

Recently, changes in cerebral  $O_2Hb$  and  $HHb$  were compared to corresponding changes in CBF and CBV as measured by positron emission tomography (PET) (Rostrup et al., 2002). Changes in CBV measured with both techniques were significantly correlated to  $CO_2$  levels. However,  $\Delta CBV(NIRS)$  was much smaller than  $\Delta CBV(PET)$ . Rostrup et al. (2002) concluded that while qualitatively correct, NIRS measurements of CBV should be used with caution when quantitative results are needed.

### **Cortical Activation (Functional NIRS)**

Neuroimaging techniques, such as functional MRI (fMRI) and PET, monitor task-related neuronal activations in the brain indirectly through the associated neurovascular/metabolic responses. fMRI and PET measure local changes in brain hemodynamics induced by motor, visual, cognitive, or perceptual tasks. Moreover, fMRI and PET measures are characterised by a uniform highly spatial resolution (millimetres or less) and a poor temporal resolution (about 1 s). Conversely, EEG, magnetoencephalography (MEG), and NIRS measure instantaneously the current flows induced by synaptic activity or the cortical hemodynamics. Recently techniques have been developed that, in the context of brain anatomy visualized with structural MRI, use both hemodynamic and electromagnetic measures to arrive at estimates of brain activation with high spatial and temporal resolution. These methods range from simple juxtaposition to simultaneous integrated techniques. Their application has already led to advances in our understanding of the neural bases of perception, attention, memory, language, etc. Further advances in multi-modality integration will require a better understanding of the coupling between the physiological phenomena underlying the different signal modalities.

NIR optical topography is the simultaneous acquisition of  $O_2Hb$  and  $HHb$  changes from an array of optical fibers on the scalp to construct maps of cortical activity. The oxygenation response typically expected over an activated cortical area consists of a decrease in  $HHb$  accompanied with an increase in  $O_2Hb$  of two- to threefold of magnitude. NIRS and fMRI both allow noninvasive monitoring of cerebral cortical  $HHb$  responses to various stimuli. Kleinschmidt et al. (1996) first measured simultaneously cerebral oxygenation changes during human brain motor activation by fMRI and one-channel fNIRS. fNIRS and fMRI measurements showed good correlation in young and elderly subjects during a motor task (Mehagnoul-Schipper et al., 2002).

Toronov et al. (2001) investigated human brain hemodynamics by simultaneous NIRS and fMRI mapping during a periodic sequence of stimulation by finger motion and rest. Both methods revealed a good co-location of the brain activity centers. While rough spatial correspondences with maps generated from fMRI were found in these experiments, the amplitude correspondences between the two

recording modalities have not been fully characterized. Recently, strong correlations were found between fMRI changes and all optical measures, with O<sub>2</sub>Hb providing the strongest correlation (Strangman et al., 2002b).

NIRS has been used to monitor child and adult brain function in a wide variety of tasks. A recent review covers the literature on intrinsic optical signal and the functional brain NIRS imaging studies of the past few years (Obrig and Villringer, 2003). In this research field, Kennan et al. (2002b) demonstrated that optical topography could be used to determine lateralization of prefrontal areas to a language task that has been validated by fMRI. Kennan et al. (2002a) also demonstrated that optical topography can be used to simultaneously detect and characterize the hemodynamic responses associated with an “oddball” auditory stimulus, and that corresponding electrical event related potentials (ERP) could be acquired simultaneously using conventional scalp recordings. In addition to the measured electrical response, the hemodynamic localization was consistent with fMRI studies, which showed significant activation in the temporal and parietal cortical regions.

This study showed the regions of peak hemodynamic activity that were in closest proximity to areas of peak electrical activity. This was the first demonstration of simultaneous ERP electrical recording and noninvasive optical mapping in human subjects. The same group also demonstrated, by using a global hyperoxic or mild hypoxic challenge, that it is possible to normalize the activation response in terms of the fractional changes in CBV, tissue oxygenation index, and O<sub>2</sub> extraction ratio, which are independent of the optical pathlength (Kennan and Behar, 2002).

Maps of concentration changes in O<sub>2</sub>Hb, HHb, and tHb of the visual and motor cortices were generated via a frequency-domain NIRS during stimulation using a reversing checkerboard screen and palm-squeezing, respectively (Wolf et al., 2002c). In the visual cortex the patterns of O<sub>2</sub>Hb and HHb were linearly correlated in 13 of 24 locations. The patterns of the O<sub>2</sub>Hb and HHb traces over the motor cortex looked different. The O<sub>2</sub>Hb reached its maximum change a few seconds before the HHb reached its minimum. Patterns of O<sub>2</sub>Hb and HHb differed among cortex areas. This implies that the regulation of perfusion in the visual cortex differs from that in the motor cortex. There is evidence that the cerebral metabolic rate for O<sub>2</sub> increases substantially in the visual cortex, while this is not the case for the motor cortex (Wolf et al., 2002c).

The literature on the fast intrinsic optical signal is quite controversial (Obrig and Villringer, 2003). Millisecond changes in the optical properties of the human brain during motor stimulation were recently detected using frequency-domain NIRS (Wolf et al., 2002b). During a motor stimulation task, highly significant signals were found which were directly related to neuronal activity and exhibited much more localized patterns than the slow hemodynamic signals.

Chance et al. (1993) first reported observations of NIR absorbance changes attributable to repetitive tHb changes in response to stimulation in the human brain frontal region by a cognitive process. These responses were observed as low-frequency recurrence of changes by Fourier transform analysis. Toronov et al. (2000) studied the motor cortex hemodynamics in human subjects at rest and under motor stimulation conditions using a multichannel near-infrared tissue spectrometer (ac-

quisition time of 160 ms per map). The main findings were: (a) the amplitude of the hemodynamic response to the motor stimulation was comparable to the amplitude of the fluctuations at rest; (b) the spatial patterns of the O<sub>2</sub>Hb and HHb responses to the stimulation were different; and (c) the hemodynamic response to stimulation showed a spatial localization and a level of phase synchronization with the motor stimulation that depended on the stimulation period.

Obrig et al. (2000) investigated slow spontaneous oscillations in cerebral oxygenation in the human adult's visual cortex. Both the spectral power and the phase relationship between O<sub>2</sub>Hb and HHb were analysed. Spontaneous vascular and metabolic low frequency oscillations (LFO) centered around 0.1 s<sup>-1</sup> and very LFO (VLFO) centered around 0.004 s<sup>-1</sup> were reproducibly detected by NIRS in the human adult brain. Their respective power differed between O<sub>2</sub>Hb and HHb. Either frequency (LFO and VLFO) was altered in magnitude by functional stimulation of the cortical area examined. Their spectral characteristics and their response to hypercapnia corresponded to findings with transcranial Doppler sonography and fMRI.

Recently Fantini (2002) presented a model that describes the effect of physiological parameters such as the speed of BF, local O<sub>2</sub> consumption, capillary recruitment, and vascular dilation and constriction on Hb concentration and O<sub>2</sub> saturation in tissue. This model suggests that the superposition of asynchronous contributions from the arterial, capillary, and venous Hb compartments may be at the origin of observed out-of-phase oscillations of the O<sub>2</sub>Hb and HHb concentrations in tissue.

## Perspectives

On average, one article a day is reported on MEDLINE about the *in vivo* applications of NIRS. Most are clinical studies. However, many researchers have been using NIRS in exercise physiology (see accompanying symposium papers by Bhambhani and by Neary) and neuroscience. Since oxidative metabolism is the dominant source of energy for skeletal muscle, the possibility of investigating it noninvasively in exercising muscles and following its modification in response to specific training or rehabilitation programs is of great interest. Recently the combination of <sup>31</sup>P-MRS with NIRS has enhanced the opportunity to measure local muscle oxidative metabolism noninvasively during exercise (Binzoni et al., 1998; Boushel et al., 1998; Cerretelli et al., 1997). Moreover, NIRS in combination with surface electromyography can shed light on one of the possible causes of muscle fatigue (Miura et al., 2000). Human brain mapping is one of the key areas of neuroscience research. From this point of view, functional NIRS is giving a unique contribution considering that it has several advantages over existing technologies (MRI, PET, etc.) for brain imaging (Hoshi, 2003; Obrig and Villringer, 2003).

## Acknowledgments

This research was supported in part by the EC QLGI-CT-200-01464. We wish to thank Dr. M. Wolf for his helpful suggestions.

## References

- Al-Rawi, P.G., Smielewski, P., and Kirkpatrick, P.J. (2001). Evaluation of a near-infrared spectrometer (NIRO 300) for the detection of intracranial oxygenation changes in the adult head. **Stroke** 32: 2492-2500.
- Bangsbo, J., Krstrup, P., Gonzalez-Alonso, J., Boushel, R., and Saltin, B. (2000). Muscle oxygen kinetics at onset of intense dynamic exercise in humans. **Am. J. Physiol.** 279: R899-R906.
- Bhambhani Y. (2004). Muscle oxygenation trends during dynamic exercise measured by near infrared spectroscopy. **Can. J. Appl. Physiol.** 29: 504-523.
- Binzoni, T., Ngo, L., Girardis, M., Springett, R., Terrier, F., and Delpy, D. (2003). Venous-arteriolar reflex in human gastrocnemius studied by NIRS. **Adv. Exp. Med. Biol.** 530: 467-473.
- Binzoni, T., Quaresima, V., Barattelli, G., Hiltbrand, E., Gurke, L., Terrier, F., Cerretelli, P., and Ferrari, M. (1998). Energy metabolism and interstitial fluid displacement in human gastrocnemius during short ischemic cycles. **J. Appl. Physiol.** 85: 1244-1251.
- Binzoni, T., Quaresima, V., Ferrari, M., Hiltbrand, E., and Cerretelli, P. (2000). Human calf microvascular compliance measured by near-infrared spectroscopy. **J. Appl. Physiol.** 88: 369-372.
- Boushel, R., Langberg, H., Green, S., Skovgaard, D., Bulow, J., and Kjaer, M. (2000a). Blood flow and oxygenation in peritendinous tissue and calf muscle during dynamic exercise in humans. **J. Physiol.** 524: 305-313.
- Boushel, R., Langberg, H., Olesen, J., Gonzales-Alonzo, J., Bulow, J., and Kjaer, M. (2001). Monitoring tissue oxygen availability with near infrared spectroscopy (NIRS) in health and disease. **Scand. J. Med. Sci. Sports** 11: 213-222.
- Boushel, R., Langberg, H., Olesen, J., Nowak, M., Simonsen, L., Bulow, J., and Kjaer, M. (2000b). Regional blood flow during exercise in humans measured by near-infrared spectroscopy and indocyanine green. **J. Appl. Physiol.** 89: 1868-1878.
- Boushel, R., and Piantadosi, C.A. (2000). Near-infrared spectroscopy for monitoring muscle oxygenation. **Acta Physiol. Scand.** 168: 615-622.
- Boushel, R., Pott, F., Madsen, P., Radegran, G., Nowak, M., Quistorff, B., and Secher, N. (1998). Muscle metabolism from near infrared spectroscopy during rhythmic handgrip in humans. **Eur. J. Appl. Physiol.** 79: 41-48.
- Brown, D.W., Picot, P.A., Naeini, J.G., Springett, R., Delpy, D.T., and Lee, T.Y. (2002). Quantitative near infrared spectroscopy measurement of cerebral hemodynamics in newborn piglets. **Pediatr. Res.** 51: 564-570.
- Cerretelli, P., and Binzoni, T. The contribution of NMR, NIRS and their combination to the functional assessment of human muscle. (1997). **Int. J. Sports Med.** 18: S270-S279.
- Chance, B., Dait, M.T., Zhang, C., Hamaoka, T., and Hagerman, F. (1992). Recovery from exercise-induced desaturation in the quadriceps muscles of elite competitive rowers. **Am. J. Physiol.** 262: C766-C775.
- Chance, B., Zhuang, Z., UnAh, C., Alter, C., and Lipton, L. (1993). Cognition-activated low-frequency modulation of light absorption in human brain. **Proc. Natl. Acad. Sci. USA** 90: 3770-3774.
- Colier, W.N., Meeuwse, I.B., Degens, H., and Oeseburg, B. (1995). Determination of oxygen consumption in muscle during exercise using near infrared spectroscopy. **Acta Anaesthesiol. Scand. Suppl.** 107: 151-155.

- Conley, K.E., Ordway, G.A., and Richardson, R.S. (2000). Deciphering the mysteries of myoglobin in striated muscle. **Acta Physiol. Scand.** 168: 623-634.
- Cooper, C.E., Cope, M., Springett, R., Amess, P.N., Penrice, J., Tyszczyk, L., Punwani, S., Ordidge, R., Wyatt, J., and Delpy, D.T. (1999). Use of mitochondrial inhibitors to demonstrate that cytochrome oxidase near-infrared spectroscopy can measure mitochondrial dysfunction noninvasively in the brain. **J. Cereb. Blood Flow Metab.** 19: 27-38.
- Costes, F., Barthelemy, J.C., Feasson, L., Busso, T., Geysant, A., and Denis, C. (1996). Comparison of muscle near-infrared spectroscopy and femoral blood gases during steady-state exercise in humans. **J. Appl. Physiol.** 80: 1345-1350.
- Cubeddu, R., Biscotti, G., Pifferi, A., Taroni, P., Torricelli, A., Ferrari, M., and Quaresima, V. (2002, Oct. 21-23). Dual-wavelength, 8-channel time-resolved oximetry for functional muscle studies. **Proc. Asian Symposium on Biomedical Optics and Photomedicine**, pp 198-199. Hokkaido, Sapporo (Japan), Abs. MC3P12.
- De Blasi, R.A., Almenröder, N., and Ferrari, M. (1997). Comparison of two methods of measurement of forearm oxygen consumption by near infrared spectroscopy. **J. Biomed. Optics** 2: 171-175.
- De Blasi, R.A., Cope, M., Elwell, C., Safoue, F., and Ferrari, M. (1993). Noninvasive measurement of human forearm oxygen consumption by near infrared spectroscopy. **Eur. J. Appl. Physiol.** 67: 20-25.
- De Blasi, R.A., Ferrari, M., Natali, A., Conti, G., Mega, A., and Gasparetto, A. (1994). Noninvasive measurement of forearm blood flow and oxygen consumption by near-infrared spectroscopy. **J. Appl. Physiol.** 76: 1388-1393.
- Delpy, D.T., and Cope, M. (1997). Quantification in tissue near-infrared spectroscopy. **Philos. Trans. R. Soc. Lond. B. Biol. Sci.** 352: 649-659.
- De Visscher, G., Springett, R., Delpy, D.T., Van Reempts, J., Borgers, M., and van Rossem, K. (2002). Nitric oxide does not inhibit cerebral cytochrome oxidase in vivo or in the reactive hyperemic phase after brief anoxia in the adult rat. **J. Cereb. Blood Flow Metab.** 22: 515-519.
- Fantini, S. (2002). A haemodynamic model for the physiological interpretation of in vivo measurements of the concentration and oxygen saturation of haemoglobin. **Phys. Med. Biol.** 47: N249-N257.
- Ferrari, M., Binzoni, T., and Quaresima, V. (1997). Oxidative metabolism in muscle. **Philos. Trans. R. Soc. Lond. B. Biol. Sci.** 352: 677-683.
- Ferrari, M., Wei, Q., Carraresi, L., De Blasi, R.A., and Zaccanti, G. (1992). Time-resolved spectroscopy of the human forearm. **J. Photochem. Photobiol. B.** 16: 141-153.
- Franceschini, M.A., Boas, D.A., Zourabian, A., Diamond, S.G., Nadgir, S., Lin, D.W., Moore, J.B., and Fantini, S. (2002). Near-infrared spirometry: Non-invasive measurements of venous saturation in piglets and human subjects. **J. Appl. Physiol.** 92: 372-384.
- Gora, F., Shinde, S., Elwell, C.E., Goldstone, J.C., Cope, M., Delpy, D.T., and Smith, M. (2002). Noninvasive measurement of cerebral blood flow in adults using near-infrared spectroscopy and indocyanine green: A pilot study. **J. Neurosurg. Anesthesiol.** 14: 218-222.
- Grassi B., Pogliaghi, S., Rampichini, S., Quaresima, V., Ferrari, M., Marconi, C., and Cerretelli, P. (2003). Muscle oxygenation and pulmonary gas exchange kinetics during cycling exercise on-transitions in humans. **J. Appl. Physiol.** 95: 149-158.
- Grassi, B., Quaresima, V., Marconi, C., Ferrari, M., and Cerretelli, P. (1999). Blood lactate

- accumulation and muscle deoxygenation during incremental exercise. **J. Appl. Physiol.** 87: 348-355.
- Hamaoka, T., Iwane, H., Shimomitsu, T., Katsumura, T., Murase, N., Nishio, S., Osada, T., Kurosawa, Y., and Chance, B. (1996). Noninvasive measures of oxidative metabolism on working human muscles by near-infrared spectroscopy. **J. Appl. Physiol.** 81: 1410-1417.
- Hebden, J.C., Gibson, A., Yusof, R.M., Everdell, N., Hillman, E.M., Delpy, D.T., Arridge, S.R., Austin, T., Meek, J.H., and Wyatt, J.S. (2002). Three-dimensional optical tomography of the premature infant brain. **Phys. Med. Biol.** 47: 4155-4166.
- Hicks, A., McGill, S., and Hughson, R.L. (1999). Tissue oxygenation by near-infrared spectroscopy and muscle blood flow during isometric contractions of the forearm. **Can. J. Appl. Physiol.** 24: 216-230.
- Hillman, E.M., Hebden, J.C., Schweiger, M., Dehghani, H., Schmidt, F.E., Delpy, D.T., Arridge, S.R. (2001). Time resolved optical tomography of the human forearm. **Phys. Med. Biol.** 46: 1117-1130.
- Homma, S., Eda, H., Ogasawara, S., and Kagaya, A. (1996). Near-infrared estimation of O<sub>2</sub> supply and consumption in forearm muscles working at varying intensity. **J. Appl. Physiol.** 80: 1279-1284.
- Hopton, P., Walsh, T.S., and Lee, A. (1999). Measurement of cerebral blood volume using near-infrared spectroscopy and indocyanine green elimination. **J. Appl. Physiol.** 87: 1981-1987.
- Hoshi, Y. (2003). Functional near-infrared optical imaging: Utility and limitations in human brain mapping. **Psychophysiol.** 40: 511-520.
- Hoshi, Y., Hazeki, O., Kakhana, and Y., Tamura, M. (1997). Redox behavior of cytochrome oxidase in the rat brain measured by near-infrared spectroscopy. **J. Appl. Physiol.** 83: 1842-1848.
- Hoshi, Y., Oda, I., Wada, Y., Ito, Y., Yamashita, Y., Oda, M., Ohta, K., Yamada, Y., and Tamura, M. (2000). Visuospatial imagery is a fruitful strategy for the digit span backward task: A study with near-infrared optical tomography. **Brain Res. Cogn. Brain Res.** 9: 339-342.
- Imray, C.H., Barnett, N.J., Walsh, S., Clarke, T., Morgan, J., Hale, D., Hoar, H., Mole, D., Chesner, I., and Wright, A.D. (1998). Near-infrared spectroscopy in the assessment of cerebral oxygenation at high altitude. **Wilderness Environ. Med.** 9: 198-203.
- Jobsis, F.F. (1977). Noninvasive, infrared monitoring of cerebral and myocardial oxygen sufficiency and circulatory parameters. **Science** 198: 1264-1267.
- Kennan, R.P., and Behar, K.L. (2002). Continuous-wave near-infrared spectroscopy using pathlength-independent hypoxia normalization. **J. Biomed. Opt.** 7: 228-235.
- Kennan, R.P., Horowitz, S.G., Maki, A., Yamashita, Y., Koizumi, H., and Gore, J.C. (2002a). Simultaneous recording of event-related auditory oddball response using transcranial near infrared optical topography and surface EEG. **Neuroimage** 16: 587-592.
- Kennan, R.P., Kim, D., Maki, A., Koizumi, H., and Constable R.T. (2002b). Non-invasive assessment of language lateralization by transcranial near infrared optical topography and functional MRI. **Hum. Brain Mapp.** 16: 183-189.
- Kleinschmidt, A., Obrig, H., Requardt, M., Merboldt, K.D., Dirnagl, U., Villringer, A., and Frahm, J. (1996). Simultaneous recording of cerebral blood oxygenation changes during human brain activation by magnetic resonance imaging and near-infrared spectroscopy. **J. Cereb. Blood Flow Metab.** 16: 817-826.



- Kohl-Bareis, M., Obrig, H., Steinbrink, J., Malak, J., Uludag, K., and Villringer, A. (2002). Noninvasive monitoring of cerebral blood flow by a dye bolus method: Separation of brain from skin and skull signals. **J. Biomed. Opt.** 7: 464-470.
- Kohri, S., Hoshi, Y., Tamura, M., Kato, C., Kuge, Y., and Tamaki, N. (2002). Quantitative evaluation of the relative contribution ratio of cerebral tissue to near-infrared signals in the adult head: A preliminary study. **Physiol. Measur.** 23: 301-312.
- Komiyama, T., Quaresima, V., Shigematsu, H., and Ferrari, M. (2001). Comparison of two spatially resolved near-infrared photometers in the detection of tissue oxygen saturation: Poor reliability at very low oxygen saturation. **Clin. Sci.** 101: 715-718.
- Kusaka, T., Isobe, K., Nagano, K., Okubo, K., Yasuda, S., Kondo, M., Itoh, S., and Onishi, S. (2001). Estimation of regional cerebral blood flow distribution in infants by near-infrared topography using indocyanine green. **Neuroimage** 13: 944-952.
- MacDonald, M.J., Tarnopolsky, M.A., Green, H.J., and Hughson, R.L. (1999). Comparison of femoral blood gases and muscle near-infrared spectroscopy at exercise onset in humans. **J. Appl. Physiol.** 86: 687-693.
- Madsen, P.L., and Secher, N.H. (1999). Near-infrared oximetry of the brain. **Prog. Neurobiol.** 58: 541-560.
- Mancini, D.M., Wilson, J.R., Bolinger, L., Li, H., Kendrick, K., Chance, B., and Leigh, J.S. (1994). In vivo magnetic resonance spectroscopy measurement of deoxymyoglobin during exercise in patients with heart failure. Demonstration of abnormal muscle metabolism despite adequate oxygenation. **Circulation** 90: 500-508.
- Masuda, K., Choi, J.Y., Shimojo, H., and Katsuta, S. (1999). Maintenance of myoglobin concentration in human skeletal muscle after heavy resistance training. **Eur. J. Appl. Physiol. Occup. Physiol.** 79: 347-352.
- Matsushita, K., Homma, S., and Okada, E. (1998). Influence of adipose tissue on muscle oxygenation measurement with NIRS instrument. **Proc. SPIE** 3194: 151-165.
- McCully, K.K., and Hamaoka, T. (2000). Near-infrared spectroscopy: What can it tell us about oxygen saturation in skeletal muscle? **Exerc. Sport Sci. Rev.** 28: 123-127.
- McCully, K.K., Iotti, S., Kendrick, K., Wang, Z., Posner, J.D., Leigh, J. Jr., and Chance, B. (1994). Simultaneous in vivo measurements of HbO<sub>2</sub> saturation and PCr kinetics after exercise in normal humans. **J. Appl. Physiol.** 77: 5-10.
- Mehagnoul-Schipper, D.J., van der Kallen, B.F., Colier, W.N., van der Sluijs, M.C., van Erning, L.J., Thijssen, H.O., Oeseburg, B., Hoefnagels, W.H., and Jansen, R.W. (2002). Simultaneous measurements of cerebral oxygenation changes during brain activation by near-infrared spectroscopy and functional magnetic resonance imaging in healthy young and elderly subjects. **Hum. Brain Mapp.** 16: 14-23.
- Miura, H., Araki, H., Matoba, H., and Kitagawa, K. (2000). Relationship among oxygenation, myoelectric activity, and lactic acid accumulation in vastus lateralis muscle during exercise with constant work rate. **Int. J. Sports Med.** 21: 180-184.
- Miura, H., McCully, K., Hong, L., Nioka, S., and Chance, B. (2001). Regional difference of muscle oxygen saturation and blood volume during exercise determined by near infrared imaging device. **Jpn. J. Physiol.** 51: 599-606.
- Neary, J.P. (2004). Application of near infrared spectroscopy to exercise sports science. **Can. J. Appl. Physiol.** 29: 488-503.
- Newton, C.R., Wilson, D.A., Gunnoe, E., Wagner, B., Cope, M., and Traystman, R.J. (1997). Measurement of cerebral blood flow in dogs with near infrared spectroscopy in the reflectance mode is invalid. **J. Cereb. Blood Flow Metab.** 17: 695-703.



- Niwayama, M., Lin, L., Shao, J., Kudo, N., and Yamamoto, K. (2000). Quantitative measurement of muscle hemoglobin oxygenation using near-infrared spectroscopy with correction for the influence of a subcutaneous fat layer. **Rev. Sci. Instr.** 71: 4571-4575.
- Obrig, H., Neufang, M., Wenzel, R., Kohl, M., Steinbrink, J., Einhaupl, K., and Villringer, A. (2000). Spontaneous low frequency oscillations of cerebral hemodynamics and metabolism in human adults. **Neuroimage** 12: 623-639.
- Obrig, H., and Villringer, A. (2003). Beyond the visible-imaging the human brain with light. **J. Cereb. Blood Flow Metab.** 23: 1-18.
- Oda, M., Yamashita, Y., Nakano, T., Suzuki, A., Shimizu, K., Hirano, I., Shimomura, F., Ohmae, E., Suzuki, T., and Tsuchiya, Y. (2000). Near infrared time-resolved spectroscopy system for tissue oxygenation monitor. **Proc. SPIE** 4160: 204-210.
- Okada, E., and Delpy, D.T. (2003). Near-infrared light propagation in an adult head model. II. Effect of superficial tissue thickness on the sensitivity of the near-infrared spectroscopy signal. **Appl. Opt.** 42: 2915-2922.
- Owen-Reece, H., Smith, M., Elwell, C.E., and Goldstone, J.C. (1999). Near infrared spectroscopy. **Br. J. Anaesth.** 82: 418-426.
- Quaresima, V., Colier, W.N., van der Sluijs, M., and Ferrari, M. (2001a). Nonuniform quadriceps O<sub>2</sub> consumption revealed by near infrared multipoint measurements. **Biochem. Biophys. Res. Commun.** 285: 1034-1039.
- Quaresima, V., Ferrari, M., van der Sluijs, M.C., Menssen, J., and Collier, W.N. (2002a). Lateral frontal cortex oxygenation changes during translation and language switching revealed by non-invasive near-infrared multi-point measurements. **Brain Res. Bull.** 59: 235-243.
- Quaresima, V., Homma, S., Azuma, K., Shimizu, S., Chiarotti, F., Ferrari, M., and Kagaya, A. (2001b). Calf and shin muscle oxygenation patterns and femoral artery blood flow during dynamic plantar flexion exercise in humans. **Eur. J. Appl. Physiol.** 84: 387-394.
- Quaresima, V., Komiyama, T., and Ferrari, M. (2002b). Differences in oxygen re-saturation of thigh and calf muscles after two treadmill stress tests. **Comp. Biochem. Physiol. A.** 132: 67-73.
- Quaresima, V., Springett, R., Cope, M., Wyatt, J.T., Delpy, D.T., Ferrari, M., and Cooper, C.E. (1998). Oxidation and reduction of cytochrome oxidase in the neonatal brain observed by in vivo near-infrared spectroscopy. **Biochim. Biophys. Acta** 1366: 291-300.
- Richardson, R.S., Noyszewski, E.A., Saltin, B., and Gonzalez-Alonso, J. (2002). Effect of mild carboxy-hemoglobin on exercising skeletal muscle: Intravascular and intracellular evidence. **Am. J. Physiol.** 283: R1131-R1139.
- Roberts, I.G., Fallon, P., Kirkham, F.J., Kirshbom, P.M., Cooper, C.E., Elliott, M.J., and Edwards, A.D. (1998). Measurement of cerebral blood flow during cardiopulmonary bypass with near-infrared spectroscopy. **J. Thorac. Cardiovasc. Surg.** 115: 94-102.
- Rolfe, P. (2000). In vivo near-infrared spectroscopy. **Annu. Rev. Biomed. Eng.** 2: 715-754.
- Rostrup, E., Law, I., Pott, F., Ide, K., and Knudsen, G.M. (2002). Cerebral hemodynamics measured with simultaneous PET and near-infrared spectroscopy in humans. **Brain Res.** 954: 183-193.
- Sahlin, K. (1992). Non-invasive measurements of O<sub>2</sub> availability in human skeletal muscle with near-infrared spectroscopy. **Int. J. Sports Med.** 13: S157-S160.

- Sakamoto, T., Jonas, R.A., Stock, U.A., Hatsuoka, S., Cope, M., Springett, R.J., and Nollert, G. (2001). Utility and limitations of near-infrared spectroscopy during cardiopulmonary bypass in a piglet model. **Pediatr. Res.** 49: 770-776.
- Sako, T., Hamaoka, T., Higuchi, H., Kurosawa, Y., and Katsumura, T. (2001). Validity of NIR spectroscopy for quantitatively measuring muscle oxidative metabolic rate in exercise. **J. Appl. Physiol.** 90: 338-344.
- Shiga, T., Tanabe, K., Nakase, Y., Shida, T., and Chance, B. (1995). Development of a portable tissue oximeter using near infrared spectroscopy. **Med. Biol. Eng. Comput.** 33: 622-626.
- Springett, R., Newman, J., Cope, M., and Delpy, D.T. (2000a). Oxygen dependency and precision of cytochrome oxidase signal from full spectral NIRS of the piglet brain. **Am. J. Physiol.** 279: H2202-H2209.
- Springett, R., Sakata, Y., and Delpy, D.T. (2001). Precise measurement of cerebral blood flow in newborn piglets from the bolus passage of indocyanine green. **Phys. Med. Biol.** 46: 2209-2225.
- Springett, R., Wylezinska, M., Cady, E.B., Cope, M., and Delpy, D.T. (2000b). Oxygen dependency of cerebral oxidative phosphorylation in newborn piglets. **J. Cereb. Blood Flow Metab.** 20: 280-289.
- Strangman, G., Boas, D.A., and Sutton, J.P. (2002a). Non-invasive neuroimaging using near-infrared light. **Biol. Psychiatry** 52: 679-693.
- Strangman, G., Culver, J.P., Thompson, J.H., and Boas D.A. (2002b). A quantitative comparison of simultaneous BOLD fMRI and NIRS recordings during functional brain activation. **Neuroimage** 17: 719-731.
- Suzuki, S., Takasaki, S., Ozaki, T., and Kobayashi, Y. (1999). A tissue oxygenation monitor using NIR spatially resolved spectroscopy. **Proc. SPIE** 3597: 582-592.
- Thavasothy, M., Broadhead, M., Elwell, C., Peters, M., and Smith, M. (2002). A comparison of cerebral oxygenation as measured by the NIRO 300 and the INVOS 5100 Near-infrared spectrophotometers. **Anaesthesia** 57: 999-1006.
- Toronov, V., Franceschini, M.A., Filiaci, M., Fantini, S., Wolf, M., Michalos, A., and Gratton, E. (2000). Near-infrared study of fluctuations in cerebral hemodynamics during rest and motor stimulation: Temporal analysis and spatial mapping. **Med. Phys.** 27: 801-815.
- Toronov, V., Webb, A., Choi, J.H., Wolf, M., Michalos, A., Gratton, E., and Hueber, D. (2001). Investigation of human brain hemodynamics by simultaneous near-infrared spectroscopy and functional magnetic resonance imaging. **Med. Phys.** 28: 521-527.
- Tran, T.K., Sailasuta, N., Kreuzer, U., Hurd, R., Chung, Y., Mole, P., Kuno, S., and Jue, T. (1999). Comparative analysis of NMR and NIRS measurements of intracellular PO<sub>2</sub> in human skeletal muscle. **Am. J. Physiol.** 276: R1682-R1690.
- Uludag, K., Kohl, M., Steinbrink, J., Obrig, H., and Villringer, A. (2002). Cross talk in the Lambert-Beer calculation for near-infrared wavelengths estimated by Monte Carlo simulations. **J. Biomed. Opt.** 7: 51-59.
- van Beekvelt, M.C., Borghuis, M.S., van Engelen, B.G., Wevers, R.A., and Colier, W.N. (2001a). Adipose tissue thickness affects in vivo quantitative near-IR spectroscopy in human skeletal muscle. **Clin. Sci.** 101: 21-28.
- van Beekvelt, M.C., Colier, W.N., Wevers, R.A., and Van Engelen, B.G. (2001b). Performance of near-infrared spectroscopy in measuring local O<sub>2</sub> consumption and blood flow in skeletal muscle. **J. Appl. Physiol.** 90: 511-519.

- van Beekvelt, M.C.P., van Engelen, B.G.M., Wevers, R.A., and Colier, W.N.J.M. (2002). *In vivo* quantitative near-infrared spectroscopy in skeletal muscle during incremental isometric handgrip exercise. **Clin. Physiol. & Funct. Im.** 22: 210-217.
- van de Ven, M.J., Colier, W.N., van der Sluijs, M.C., Walraven, D., Oeseburg, B., and Folgering, H. (2001). Can cerebral blood volume be measured reproducibly with an improved near infrared spectroscopy system? **J. Cereb. Blood Flow Metab.** 21: 110-113.
- van Lieshout, J.J., Wieling, W., Karemaker, J.M., and Secher, N.H. (2003) Syncope, cerebral perfusion, and oxygenation. **J. Appl. Physiol.** 94: 833-848.
- Wittenberg J.B., and Wittenberg, B.A. (2003). Myoglobin function reassessed. **J. Exp. Biol.** 206: 2011-2020.
- Wobst, P., Wenzel, R., Kohl, M., Obrig, H., and Villringer, A. (2001). Linear aspects of changes in deoxygenated hemoglobin concentration and cytochrome oxidase oxidation during brain activation. **Neuroimage** 13: 520-530.
- Wolf, M., von Siebenthal, K., Keel, M., Dietz, V., Baenziger, O., and Bucher, H.U. (2002a). Comparison of three methods to measure absolute cerebral hemoglobin concentration in neonates by near-infrared spectrophotometry. **J. Biomed. Opt.** 7: 221-227.
- Wolf, M., Wolf, U., Choi, J.H., Gupta, R., Safonova, L.P., Paunescu, L.A., Michalos, A., and Gratton, E. (2002b). Functional frequency-domain near-infrared spectroscopy detects fast neuronal signal in the motor cortex. **Neuroimage** 16: 1868-1875.
- Wolf, M., Wolf, U., Toronov, V., Michalos, A., Paunescu, L.A., Choi, J.H., and Gratton, E. (2002c). Different time evolution of oxyhemoglobin and deoxyhemoglobin concentration changes in the visual and motor cortices during functional stimulation: A near-infrared spectroscopy study. **Neuroimage** 16: 704-712.
- Yoxall, C.W., and Weindling, A.M. (1997). Measurement of venous oxyhaemoglobin saturation in the adult human forearm by near infrared spectroscopy with venous occlusion. **Med. Biol. Eng. Comput.** 35: 331-336.
- Zhao, H., Tanikawa, Y., Gao, F., Onodera, Y., Sassaroli, A., Tanaka, K., and Yamada, Y. (2002). Maps of optical differential pathlength factor of human adult forehead, somatosensory motor and occipital regions at multi-wavelengths in NIR. **Phys. Med. Biol.** 47: 2075-2093.

*Received July 4, 2003; accepted in final form February 17, 2004.*